Skeleton-Based Abdominal Aorta Registration Technique

C. Feinen[1] and J. Czajkowska[1,2] and M. Grzegorzek[1] and M. Raspe[3], and R. Wickenhöfer[4]

Abstract— **Vascular diseases are the most challenging health problems in developed countries. The vascular segmentation as well as registration techniques are the topics of past and on-going research activities. In this work we target an abdominal aorta registration technique. The developed methodology is useful in the assessment of abdominal aortic aneurysm treatment by visualizing the correspondence between pre- and post-operative Computed Tomography (CT) data. The presented approach makes it possible to match all voxels belonging to the aorta from different CT series. It is based on aorta lumen segmentation and graph matching method. To segment the lumen area a hybrid level-set active contour approach is used. The matching step is performed based on a path similarity skeleton graph matching procedure. The registration results have been tested on the database of 8 patients, for which two different contrast-enhanced CT series were acquired. All registration results achieved with our system and verified by an expert prove the efficiency of the approach and encourage to further develop this method.**

I. INTRODUCTION

Nowadays, vascular diseases belong to the most challenging health problems in developed countries. An abdominal aortic aneurysm (AAA), addressed in our approach, is a dilated and weakened segment of the abdominal aorta. It is an abnormal ballooning of the abdominal portion of the aorta, that occurs as a consequence of aortic medial degeneration and can break open causing death. To prevent from rupturing, interventional radiologists offer minimally invasive treatment for abdominal aortic aneurysm. The open surgical repair by a vascular surgeon is the most commonly used for a large, non-ruptured aneurysm. The less invasive and relatively new technique, eliminating the need for a large abdominal incision, is placing a graft within the aneurysm. It redirects blood flow and stops direct pressure from being exerted on the weak aortic wall [1].

A contrast-enhanced CT angiography (CTA) is an imaging technique commonly used in vascular diagnosis. Despite the fast development of modern contrast-enhanced Computed Tomography (CT) the tremendous amount of problems still remain unsolved. The vascular segmentation [2] and registration techniques are the topics of past as well as on-going research activities.

The newest approaches in AAA segmentation are [2], [3], [4]. An pseudo 3D method for the segmentation of thrombus in abdominal aortic aneurysms from CTA data is presented in [3]. The full 3D segmentation technique in CTA is given in [4]. As reported in [2] the current state of the art in AAA segmentation is modelling, feature analysis or their combination.

Despite the fact that the segmentation of vascular structures is valuable for diagnosis assistance, treatment and surgery planning, the currently developed computer aided diagnosis (CAD) software targets in efficient image registration. It allows combining different image information (pre- and post-operative CTA studies), which is useful for treatment planning and monitoring.

The authors of [7] propose a registration technique based on the overlaying the pre-operative 3D model of the aorta onto the intra-operative 2D X-ray images. The 2D/3D registration technique is also addressed in [5]. The non-rigid method enables information from the CT to be overlaid onto the fluoroscopy images during the implantation procedure. The automatic movement compensation in 2D/3D registration of fluoroscopy and pre-operative volumetric data is presented in [8]. The idea of a 2D/3D graph-based approach in this context is presented in [6], where the algorithm takes the 3D graph generated from a segmented CT volume and the 2D distance map calculated from the 2D X-ray image. For computing the graph similarity, different measures are then used in a length preservation and a smoothness regularization term.

In this work we focus on a 3D abdominal aortic aneurysm registration technique. The developed approach makes it possible to match the aorta segmented in pre- and post-operative CTA data. The presented technique is based on an aorta lumen segmentation and graph matching technique. In the segmentation step a hybrid level-set active contour approach is employed. The applied hybrid medical image segmentation method in the level-set framework [10] uses the object's boundary as well as region information. The matching step is performed based on a path similarity skeleton graph matching procedure presented in [14]. The introduced modification to this state of the art technique incorporates the location of three characteristic points in the series, which makes it possible to properly orient the analysed skeleton end points.

*This work was funded by the German Research Foundation (DFG) as part of the research training group GRK 1564 "Imaging New Modalities". The research is supported by the NCN Grant no. UMO-2012/05/B/ST7/02136. The experimental data was provided by SOVAmed GmbH: www.sovamed.com/en

[1]J. Czajkowska, C. Feinen and M. Grzegorzek are with Research Group for Pattern Recognition, Institute for Vision and Graphics, University of Siegen, Hoelderlinstr. 3, 57076 Siegen, Germany christian.feinen@uni-siegen.de, marcin.grzegorzek@uni-siegen.de

[2]J. Czajkowska is with Department of Informatics and Medical Equipment, Faculty of Biomedical Engineering, Silesian University of Technology, ul. Charlesa de Gaulle'a 66, 41-800 Zabrze, Poland jczajkowska at polsl.pl

[3]M. Raspe is with SOVAmed GmbH, Universitaetstr. 3, 56070 Koblenz,

[4]R. Wickenhöfer is with Herz-Jesu-Krankenhaus, Südring 8, 56428 Dernbach

978-1-4244-7929-0/14/$26.00 ©2014 IEEE

In the following section, an applied algorithm for AAA lumen segmentation is presented. Section III describes the 3D skeletonisation algorithm for graph extraction and Section IV introduces the graph matching technique. Section V presents the experiments and the obtained results. With Section VI) we conclude our work and outline plans for the future.

II. ABDOMINAL AORTA SEGMENTATION TECHNIQUE

a) Aorta: To segment the aorta in CTA series a hybrid active contour method [10] is incorporated. The active contour C is represented by the zero set of embedding function ϕ, such that $C = \{x|\phi(x) = 0\}$. The points inside and outside the contour have positive and negative ϕ values, respectively. The minimized functional in image I domain Ω is defined as

$$E(\phi) = -\omega \int_{\Omega} (I - \mu) H(\phi) d\Omega + \eta \int_{\Omega} g |\nabla H(\phi)| d\Omega, \quad (1)$$

where $g = g(|\nabla I|)$ is a boundary feature map related to the image gradient and H stands for a Heaviside function. The parameters ω and η balance the two terms of (1), and μ indicates the lower bound of the gray-level of the target object. Thanks to it, the curve evolves to enclose the regions greater than μ. The Partial Differential Equation (PDE) of the functional (1) is derived from the Gateaux derivative gradient flow [10]

$$\phi_t = |\nabla \phi| \left[\omega (I - \mu) + \eta div \left(g \frac{\nabla \phi}{|\nabla \phi|} \right) \right], \quad (2)$$

and the explicit curve evolution PDE is represented by [10]

$$C_t = \omega (I - \mu) \overrightarrow{N} - \eta \langle \nabla g \cdot \overrightarrow{N} \rangle \overrightarrow{N} + \eta g \kappa \overrightarrow{N}, \quad (3)$$

where the index t denotes a time. The direction of the curve normal $\overrightarrow{N}$ is defined to point outward the curve and $\overrightarrow{N} = -\frac{\nabla \phi}{|\nabla \phi|}$. The curvature κ is given by $\kappa = div \left(\frac{\nabla \phi}{|\nabla \phi|} \right)$. The used iterative curve evolution algorithm, based on additive operator splitting (AOS) approach is in detail described in [10].

In the hybrid level-set implementation applied to volumetric CT data, the authors of [10] used a sphere as an initial surface. The results presented by them show that it successfully converges to the target object. However, the performed experiments proved, that the time to converge the hybrid level-set algorithm [10] strongly depends on this surface. In our work, the size of the analysed AAA CTA data ($512 \times 512 \times n$, where $n \in [220, 680]$) determined the clustering-based initial surface selection procedure. For this, we used a weighted fuzzy c-means clustering procedure introduced in [11].

b) Kidneys and Spine: For the actual graph matching process, further organs are required which operate as anchor points in 3D. For this task, the two Kidneys as well as L4 of the lumbar spine are chosen as reference points. In order to segment these organs a clustering based technique [11] is applied. The introduction of these three points is drastically important, since it offers us a plenty of great possibilities for all subsequent steps, e.g., they can be used to create a local object coordinate system which can be used to be rotation invariant. Moreover, the points create a unique plane $\mathcal{K}$ in 3D allowing to establish highly robust sample point relations (cf. Section IV). The 3D segmentation results and the correspondence are given in Fig. 1.

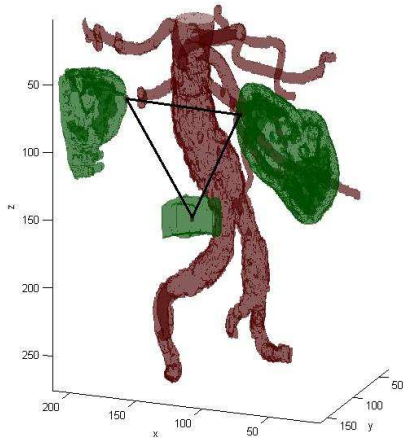

Fig. 1. 3D segmentation results of segmented organs with three characteristic points in the series used for the further skeleton matching step.

III. SKELETONISATION

The CTA volume matching procedure, being the overall goal of our work, is based on the graph matching step described in the next section. For this purpose 3D skeleton are required which are obtained by using the method described in [12]. This automatic algorithm generates a subvoxel precise skeleton based on a subvoxel precise distance field. This means, it is able to compute accurate, precise and centred 3D curve skeletons also for objects that are less than one voxel thick. The input for the skeletonisation method described in [12] is a subvoxel precise distance field. Therefore, the isosurface yielding the object's true boundary is created based on the previously obtained segmentation results and subsequently passed to the method. Having an implicit representation of the boundary, we estimate the subvoxel precise Euclidean distance transform for n-dimensional data [13]. The resulting distance map is used to find the point with the largest distance from the boundary as well as to determine a speed image that is used as input for the fast matching propagation (FMP) step. The point at the global maximum distance from the object's boundary is calculated in a single pass through the distance field. It constitutes the start point for the FMP algorithm, in which the obtained speed image is used. The FMP is also augmented to calculate the geodesic distance (Manhattan distance) inside the object. Further branch points are then estimated based on the obtained results. Therefore, the furthest point of the model from the global maximum distance point is taken as start point of the branch. All remaining points of the branch are determined by performing a gradient descent, back-tracking procedure on the fast marching time-crossing

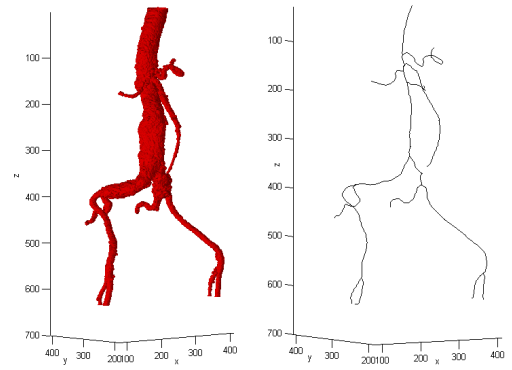

Fig. 2. An example of segmented aorta lumen and its skeleton.

map. This process is repeated for each branch of the created skeleton [13]. An exemplary result of this method that is applied to our AAA data is shown in Fig. 2.

IV. GRAPH MATCHING

The previously obtained aorta curve skeletons are now matched to properly register the two analysed 3D CTA series for each examination. Therefore, two different matching algorithm are compared to each other. The first one is the well-known Hungarian algorithm capable to find correspondences in a bipartite graph. The second matching procedure is focussing on finding *maximal weight cliques* based on an undirected weighted affinity graph G [15]. Both approaches are employed as part of path similarity skeleton graph matching presented in [14]. In more detail, the idea is to match the skeleton graphs by comparing the geodesic paths between their endpoints. In contrast to existing approaches, the authors do not explicitly consider the topological structure of the skeleton trees or graphs. Finally, the Bai et al. employ the Hungarian algorithm to calculate the overall similarity between two 2D shapes. In this work, we also utilise the Hungarian algorithm for our 3D aorta curve skeleton matching. However, caused by the higher degree of freedom in 3D, resolution variations (appearing or disappearing vessel branches) and different length ratios, we have been force to improve the method to these demands.

According to the definition given in [14], a so called skeleton path is "a shortest path between a pair of end nodes on a skeleton graph". All skeleton paths are required to be represented somehow in order to estimate their dissimilarity and thus, the matching costs for two skeleton end nodes $v \in G$ and $u \in G'$ (G denotes the query and G' the target object). Therefore, the skeleton path $p(v,u)$ is sampled by K equidistantly distributed points to compute the radius to the contour at each of these locations. In context of our work the radii are replaced by a more sophisticated description. This means, we establish relations to other organs, namely to the two kidneys $(\mathbf{k}_1, \mathbf{k}_2)$ and to the human spine $(\mathbf{m})$. Section II shortly describes how to obtain these points. Subsequently, each sample point $\mathbf{s}_i^{(v,u)}$ is described in relation to these reference points. Therefore, angles $s_i^{(v,u)} = (\alpha_i^{(v,u)}, \beta_i^{(v,u)}, \gamma_i^{(v,u)}, \delta_i^{(v,u)})$ are extracted in respect to two the direction vectors $\mathbf{v}_1 = \mathbf{k}_1 - \mathbf{m},\ \mathbf{v}_2 = \mathbf{k}_2 - \mathbf{m}$ and the normal vector $\mathbf{n_0} = \mathbf{v}_1 \times \mathbf{v}_2$ describing the plane $\mathcal{K}$ as well as the local coordinate system (LCS) of the object:

$$\begin{aligned} \alpha_i &= \arccos(\langle \hat{\mathbf{v}}_1, \hat{\mathbf{s}}_i^{(v,u)} \rangle) \\ \beta_i &= \arccos(\langle \hat{\mathbf{v}}_2, \hat{\mathbf{s}}_i^{(v,u)} \rangle) \\ \gamma_i &= \arccos(\langle \hat{\mathbf{n}}_0, \hat{\mathbf{s}}_i^{(v,u)} \rangle) \\ \delta_i &= \Psi(\langle \hat{\mathbf{v}}_1, \hat{\mathbf{s}}_i^{(v,u)} \rangle, \langle \hat{\mathbf{v}}_2, \hat{\mathbf{s}}_i^{(v,u)} \rangle), \end{aligned} \tag{4}$$

where $\hat{\mathbf{v}}_i, \hat{\mathbf{s}}_i$ and $\hat{\mathbf{n}}_0$ are unit vectors of $\mathbf{v}_i, \mathbf{s}_i, \mathbf{n}_0$ and:

$$\Psi(a,b) = \begin{cases} \arctan(a/b) & b > 0 \\ \arctan(a/b) + \pi & a \geq 0, b < 0 \\ \arctan(a/b) - \pi & a < 0, b < 0 \\ +\pi/2 & a > 0, b = 0 \\ -\pi/2 & a < 0, b = 0 \end{cases}. \tag{5}$$

This representation is invariant to rotation and scale variations. For the actual matching procedure, all s_i values are stored in a path signature vector $r^{(v,u)} = (s_1, \ldots, s_{i-1}, s_i)$. To define the dissimilarity between two skeleton paths $p^{(v,u)}$ and $p^{(v',u')}$ the authors of [14] suggest a path distance measure based on the radii and path lengths. In our work, we adapt this distance measure as follows:

$$\begin{aligned} p_d(p^{(v,u)}, p^{(v',u')}) = \ & \Phi(r^\alpha, r^\alpha) + \Phi(r^\beta, r^\beta) + \\ & \Phi(r^\gamma, r^\gamma) + \Phi(r^\delta, r^\delta), \end{aligned} \tag{6}$$

where Φ performs a dynamic time warping on the sub parts $(\alpha, \beta, \gamma, \delta)$ of the two time series $r^{(v,u)}$ and $r^{(v',u')}$, respectively.

Let now assume that the two CTA series be described by the ordered graphs G and G' with $K+1$ and $N+1$ nodes ($K \leq N$) respectively. The matching cost $c(v,u)$ is estimated based on the paths to all other vertices in G and G' emanating from v and u. The dissimilarity value between the end nodes is estimated using the Optimal Subsequence Bijection (OSB) method introduced in [16]. The advantage of the OSB algorithm is, that it finds a subsequence a' in sequence a that best matches b' in b skipping possible outlier elements. Therefore, a matrix filled with all path distance values (Eq. 6) for two node sequences $v_{i0}, v_{i1}, \ldots, v_{iK}$ in G ($v_i = v_{i0}$) and $u_{j0}, v_{j1}, \ldots, u_{jN}$ in G' ($u_j = u_{j0}$) are generated. This matrix is passed to the OSB that calculates the matching costs for the end nodes v_i and u_j. All node pairs of G and G' are analysed in this way and their OSB output values are stored in a further matrix $C^{(G,G')}$. The total dissimilarity $c(G,G')$ between G and G' is then computed in analogy to [14] with the Hungarian algorithm on $C^{(G,G')}$ first.

In a second run, we replace the Hungarian algorithm by a method proposed in [15], where the authors express the matching problem as a integer quadratic program with the goal to find maximal weight cliques in undirected affinity graph $G^\star$ satisfying a certain set of constraints:

$$\max g(\mathbf{x}) = \mathbf{x}^\intercal A \mathbf{x} \quad \text{s.t.} \quad \mathbf{x}^\intercal M \mathbf{x} = 0,\ \mathbf{x} \in \{0,1\}^n, \tag{7}$$

where A is a symmetric $n \times n$ affinity matrix with $\forall i,j = 1 \ldots, n : A_{i,j} \geq 0$ and $M \in \{0,1\}^{n \times n}$ represents a

symmetric mutual exclusion constraints (mutex) matrix. The diagonal of A is populated with the elements in $C^{(G,G')}$. Since A expects similarity data, the OSB cost values have to be converted by using a Gaussian function. In order to populate the non-diagonal elements of A, a pairwise distance consistency value is generated between two assignments $u^\star = (i, i')$ and $v^\star = (j, j')$:

$$A^{(u^\star, v^\star)} = \exp\left(\frac{(d(i,j) - d(i',j'))^2}{2\sigma^2}\right), \quad (8)$$

where $d(i, j)$ calculates the Euclidean distance and σ adjusts the influence of geometric deformations on the output value. Finally, all values are normalized to $[0, 1]$ in order to remain scale invariant. The mutex matrix M monitors simple geometrical constrains, e.g., left/right in each dimension based on the object's LCS.

V. RESULTS

The presented segmentation/registration framework was tested on the database provided by the SOVAmed GmbH. It consists of 8 pairs of of CTA series to be segmented and matched. The examinations contain pre- as well as post-operative series (in total 16). Based on the normalized CTA data the number of clusters used in initial surface construction was set to 5. In the employed hybrid level-set segmentation technique [10], a boundary feature map related to the image gradient is a decreasing function g such as $g = \frac{1}{1-c|\nabla I|^2}$, with the constant c controlling the slope set to 5. The parameters required for (1) are set to $\omega = 0.5$ and $\eta = 0.2$, respectively. The proposed set-up makes it possible to efficiently segment the aorta and reference organ points in all 16 analysed series. For all the analysed pairs of volumetric data the matching algorithm based on Hungarian method as well as Maximum Weight Cliques were investigated.

The matching results were verified by an expert. A labelled skeleton points on both series were marked, so that the expert was able to verify them (see Fig. 3), by checking the real correspondences of the anatomical points. For all the analysed data sets 7 to 13 end points (depending on the series) of the skeletons to match were detected. The Hungarian matching results in 5 totally correct matches and a mean accuracy of 89% correctly matched end points (65 of 74). Much better results were obtained using the Maximum Weight Cliques technique, where in 6 of 8 series the results were totally correct and the mean accuracy was equal to 97% correctly matched points (68 of 71). The difficulties during the matching were caused by a different resolution of the series as well as length variations. To solve this problem in the future, we plan to incorporate a DICOM positioning information and context analysis.

VI. CONCLUSIONS AND FUTURE WORK

The paper presents a preliminary study in a 3D registration of abdominal aortic aneurysm in CTA. The developed method consists of 3D segmentation part and graph based registration procedure. The promising results obtained for 8 examinations consisting of 2 CTA series each encourage to further develop this technique. In our work we plan to improve the segmentation as well as registration results incorporating a context analysis of the image data.

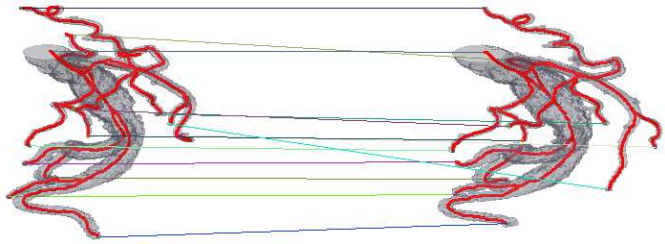

Fig. 3. An exemplary matching results with the correspondences

REFERENCES

[1] Zarins C. K., White R. A., Schwarten D., Kinney E., Diethrich E. B., Hodgson K. J., et al. AneuRx Stent Graft Versus Open Surgical Repair of Abdominal Aortic Aneurysms: Multicenter Prospective Clinical Trial. J Vascular Surg, vol.29, pp.292-308, 1999

[2] Lesage D., Angelini E. D., Bloch I., and Funka-Lea G., A review of 3D vessel lumen segmentation techniques: Models, features and extraction schemes, Medical Image Analysis, vol.13, no.6, pp.819-845, 2009

[3] de Bruijne M., van Ginneken B., Niessen W. J., Maintz J. B. A. and Viergever M. A., Active-shape-model-based segmentation of abdominal aortic aneurysms in CTA images. Proc. SPIE 4684, Medical Imaging: Image Processing, 463, May, 2002

[4] Zhuge F., Rubin G. D., Sun S. and Napel S., An abdominal aortic aneurysm segmentation method: Level set with region and statistical information, Medical Physics, vol.33, pp.1440-1453, 2006

[5] Raheem A., Carrell T., Modarai B., Penney G.: Non-rigid 2D-3D image registration for use in endovascular repair of abdominal aortic aneurysms. In: Medical Image Understanding and Analysis, pp. 153-157, 2010

[6] Liao R., Tan Y., Sundar H., Pfister M. and Kamen A., An Efficient Graph-Based Deformable 2D/3D Registration Algorithm with Applications for Abdominal Aortic Aneurysm Interventions, Medical Imaging and Augmented Reality, Lecture Notes in Computer Science, vol 6316, pp. 561-570, 2010

[7] Shun M., Liao R. and Pfister M., Toward smart utilization of two X-ray images for 2-D/3-D registration applied to abdominal aortic aneurysm interventions, BMEI2011, vol.1, no., pp.550,555, 15-17 Oct. 2011

[8] Liang D., Bo D., Shun M., Pfister M. and Rui L., Visual check and automatic compensation for patient movement during image-guided Abdominal Aortic Aneurysm (AAA) stenting, BMEI2012, pp.391-394, 16-18 Oct. 2012

[9] Sun Z., Helical CT angiography of fenestrated stent grafting of abdominal aortic aneurysms, Biomed Imaging Interv J. 2009 Apr-Jun; vol.5, no.2, 2009

[10] Zhang Y., Matuszewski B. J., Shark L.-K., Moore C. J., Medical Image Segmentation Using New Hybrid Level-Set Method, IEEE International Conference on Biomedical Visualisation, MEDi08VIS, London, pp.71-76, July, 2008

[11] Kawa, J. and Pietka, E.: *Kernelized Fuzzy C-Means Method in Fast Segmentation of Demyelination Plaques in Multiple Sclerosis*, IEEE EMBS2007, August 2007

[12] Van Uitert R. and Bitter I., Subvoxel precise skeletons of volumetric data based on fast marching methods, Medical Physics, vol. 34, no. 3, pp. 627-638, 2007

[13] Uirert R. V. and Bitter I., Subvoxel accurate Euclidean distance transforms for n-dimensional data, unpublished

[14] Bai X. and Latecki L. J., Path similarity skeleton graph matching, IEEE Transactions on Pattern Analysis and Machine Intelligence, vol 30, no. 4, pp. 1282-1292, July 2008

[15] Ma T. and Latecki L. J., Maximum weight cliques with mutex constraints for video object segmentation, IEEE CVPR, pp. 670-677. IEEE, 2012

[16] L. J. Latecki, Q. Wang, S. Koknar-Tezel, and V. Megalooikonomou, Optimal Subsequence Bijection, In ICDM, pp. 565-570, 2007